Acta Crystallographica Section F
Structural Biology and Crystallization Communications
ISSN 1744-3091
Editors: **H. M. Einspahr and M. S. Weiss**

Purification, crystallization and preliminary X-ray crystallographic analysis of the human heat-shock protein 40 Hdj1 and its C-terminal peptide-binding domain

Hironori Suzuki, Shuji Noguchi, Hiroshi Arakawa, Tadaaki Tokida, Mariko Hashimoto and Yoshinori Satow

Acta Cryst. (2010). F**66**, 1591–1595

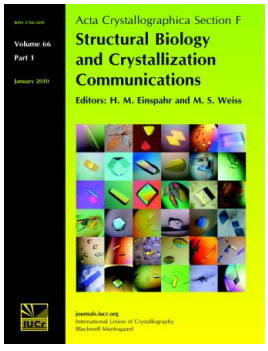

Acta Crystallographica Section F
Structural Biology and Crystallization Communications
ISSN 1744-3091

Purification, crystallization and preliminary X-ray crystallographic analysis of the human heat-shock protein 40 Hdj1 and its C-terminal peptide-binding domain

Hironori Suzuki, Shuji Noguchi, Hiroshi Arakawa, Tadaaki Tokida, Mariko Hashimoto and Yoshinori Satow*

Graduate School of Pharmaceutical Sciences, The University of Tokyo, Tokyo, Japan

Correspondence e-mail: fwkozo@mail.ecc.u-tokyo.ac.jp

Received 30 June 2010
Accepted 24 August 2010

Hsp40 is a co-chaperone of Hsp70 that correctly folds polypeptides that exist in non-native forms. The C-terminal peptide-binding domain (CTD) of the human Hsp40 Hdj1 has been purified and crystallized. In the presence of the C-terminal octapeptide of human Hsp70, four types of crystals, types I-B, II, III and IV, were grown and diffracted to 1.85, 2.51, 2.10 and 2.80 Å resolution, respectively. In the absence of the octapeptide, type I-A crystals of the CTD were grown that diffracted to 2.05 Å resolution. The full-length Hdj1 was also purified and crystallized (type V crystals); the crystal diffracted to 3.90 Å resolution.

1. Introduction

Hsp40 is a co-chaperone of Hsp70 that correctly folds polypeptides that exist in non-native forms (Frydman *et al.*, 1994). Hsp40 is also involved in important cellular processes such as protein assembly, trafficking and the suppression and degradation of non-native polypeptides (Hartl & Hayar-Hartl, 2002). Hsp40s have been classified into three types: types I, II and III (Cheetham & Caplan, 1998). All of these types of Hsp40 contain DnaJ-like domains at the N-terminus. Type I and II Hsp40s contain a C-terminal peptide-binding domain (CTD) at the C-terminus. Type I Hsp40s also contain zinc-finger domains between the DnaJ-like domain and the CTD, whereas type II Hsp40s do not. Type III Hsp40s consist of the J domain and a specialized domain such as the clathrin-binding domain found in auxilin, a mammalian neuronal-specific protein (Holstein *et al.*, 1996). During the polypeptide-folding reaction, the CTD of Hsp40 is bound to the non-native polypeptide and also to the C-terminal EEVD motif of Hsp70 (Freeman *et al.*, 1995). Hsp40 then delivers the non-native polypeptide to Hsp70 (Han & Christen, 2003) and the DnaJ-like domain of Hsp40 stimulates the ATPase activity of Hsp70 (Bukau & Horwich, 1998). Hsp70 refolds the non-native polypeptide using energy derived from ATP hydrolysis. Recently, the crystal structure of the CTD of the human type II Hsp40 Hdj1 (Lys158–Ile340) without ligands has been determined at 2.7 Å resolution (PDB entry 2qld; Hu *et al.*, 2008). However, it remains unclear how the human Hsp40 recognizes Hsp70 and the non-native polypeptide owing to a lack of structural information on human Hsp40 complexed with its ligand. To understand the co-chaperone mechanism of human Hsp40 from a structural perspective, we have purified CTDs of the type II human Hsp40 Hdj1 and crystallized these domains in both the absence and the presence of the Hsp70 C-terminal octapeptide that contains the EEVD motif. We have also purified and crystallized full-length Hdj1. Here, we report the purification and crystallization of the CTD of Hdj1 and of full-length Hdj1 and preliminary crystallographic analysis of the crystals.

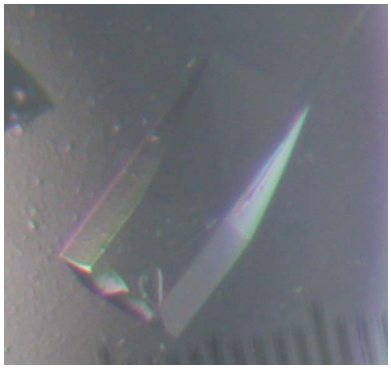

2. Experimental procedures

2.1. Expression and purification of full-length Hdj1 and the CTDs

2.1.1. Full-length Hdj1. The cDNA for Met1–Ile340 of Hdj1 was amplified by the polymerase chain reaction with KOD polymerase

(Toyobo, Tokyo, Japan) using full-length Hdj1 cDNA as the template. The PCR product was subcloned between the *Nde*I and *Sac*I sites of the pET-23a vector (Novagen, San Diego, California, USA). The recombinant plasmid was transformed into *Escherichia coli* BL21 (DE3) pLysS (Novagen) cells. The cells were pre-cultured overnight at 310 K in 100 ml LB broth containing 100 µg ml^{-1} ampicillin and 34 µg ml^{-1} chloramphenicol. The pre-cultured cells were then transferred into 7 l LB broth containing 100 µg ml^{-1} ampicillin and cultured at 310 K. The temperature was lowered to 303 K when the optical density at 600 nm reached 0.6 and isopropyl β-D-1-thio-galactopyranoside was added to a final concentration of 1 m*M*. Following 4 h of culturing, the cells were harvested by centrifugation at 12 000*g* for 10 min at 277 K, washed once with 150 m*M* NaCl solution and resuspended in lysis buffer consisting of 300 m*M* NaCl, 20 m*M* HEPES pH 7.5 and 1 m*M* phenylmethylsulfonyl fluoride (PMSF). Lysozyme (Sigma–Aldrich, St Louis, Missouri, USA) and DNase I (Nippon Gene, Tokyo, Japan) were added to the suspended solution to final concentrations of 0.2 mg ml^{-1} and 5 units ml^{-1}, respectively. The suspended cells were lysed by three freeze–thaw cycles. The lysate was centrifuged at 12 000*g* for 20 min at 277 K to remove cell debris. The Hdj1 in the supernatant solution was precipitated by ammonium sulfate between 1.0 and 1.5 *M* and collected by centrifugation at 12 000*g* for 20 min at 277 K. The collected protein was dissolved in buffer *A* (100 m*M* NaCl, 20 m*M* HEPES pH 7.5) containing 1 m*M* PMSF and dialyzed against buffer *A*. The dialyzed solution was loaded onto a 100 ml SP-Sepharose column (GE Healthcare, Piscataway, New Jersey, USA) pre-equilibrated with buffer *B* (100 m*M* NaCl, 50 m*M* HEPES pH 7.5). The column was washed with 100 ml buffer *B* and the protein was eluted with a linear NaCl gradient from 100 m*M* to 1 *M* in 360 ml buffer *B*. The eluted protein was precipitated with ammonium sulfate between 1.0 and 1.5 *M* and the precipitate was dissolved in buffer *C* (100 m*M* NaCl, 50 m*M* HEPES pH 7.0) containing 1 m*M* PMSF. The resultant solution was dialyzed against buffer *C* and loaded onto an 8 ml Mono S cation-exchange column (GE Healthcare) pre-equilibrated with buffer *C*. The loaded column was washed with 25 ml buffer *C* and Hdj1 was eluted with a linear NaCl gradient from 100 m*M* to 1 *M* in 50 ml buffer *C*. The protein sample was concentrated with an Amicon Ultra-30K concentrator (Millipore, Billerica, Massachusetts, USA) and applied onto a Superdex 200 10/30 gel-filtration column (GE Healthcare) pre-equilibrated with buffer *A*. The gel-filtration chromatogram indicated that the purified Hdj1 forms a dimer.

2.1.2. CTD$_{151–340}$. CTD$_{151–340}$ (Ser151–Leu340) was prepared from full-length Hdj1 by limited proteolysis. Bovine trypsin (Sigma–Aldrich) was added to the Hdj1 solution that had been partially purified using SP Sepharose column chromatography to a 1:24 000 trypsin:Hdj1 ratio by weight and the solution was incubated at 293 K for 1 h. The proteolysis reaction was stopped by adding 27 µ*M* *N*-α-tosyl-L-lysine chloromethyl ketone hydrochloride (Sigma–Aldrich). The trypsin-cleaved fragment was precipitated by ammonium sulfate between 1.5 and 2.0 *M* and purified using a Mono S cation-exchange column and a Superdex 75 gel-filtration column as described for the purification of Hdj1. N-terminal amino-acid sequencing and the mass-spectrometry value of 21 447 Da indicated that the trypsin-cleaved fragment was Ser151–Leu340 (the calculated molecular weight is 21 440). The gel-filtration chromatogram indicated that the purified CTD$_{151–340}$ forms a dimer.

2.1.3. CTD$_{161–340}$. The cDNA for Asp161–Ile340 of Hdj1 with an initial methionine residue at the N-terminus (CTD$_{161–340}$) was amplified by the polymerase chain reaction with KOD polymerase using full-length Hdj1 cDNA as the template. The PCR product was subcloned between the *Nde*I and *Sal*I sites of pET-23a. The resultant plasmid was transformed into *E. coli* Rosetta2 (DE3) pLysS cells (Novagen). Expression, cell lysis, purification by ammonium sulfate fractionation and SP Sepharose column chromatography were performed as described for the purification of full-length Hdj1, except that CTD$_{161–340}$ was precipitated by ammonium sulfate between 1.5 and 2.0 *M*. CTD$_{161–340}$ purified by SP Sepharose column chromatography was dialyzed against buffer *C* and loaded onto an 8 ml POROS HS cation-exchange column (PerSeptive BioSystems,

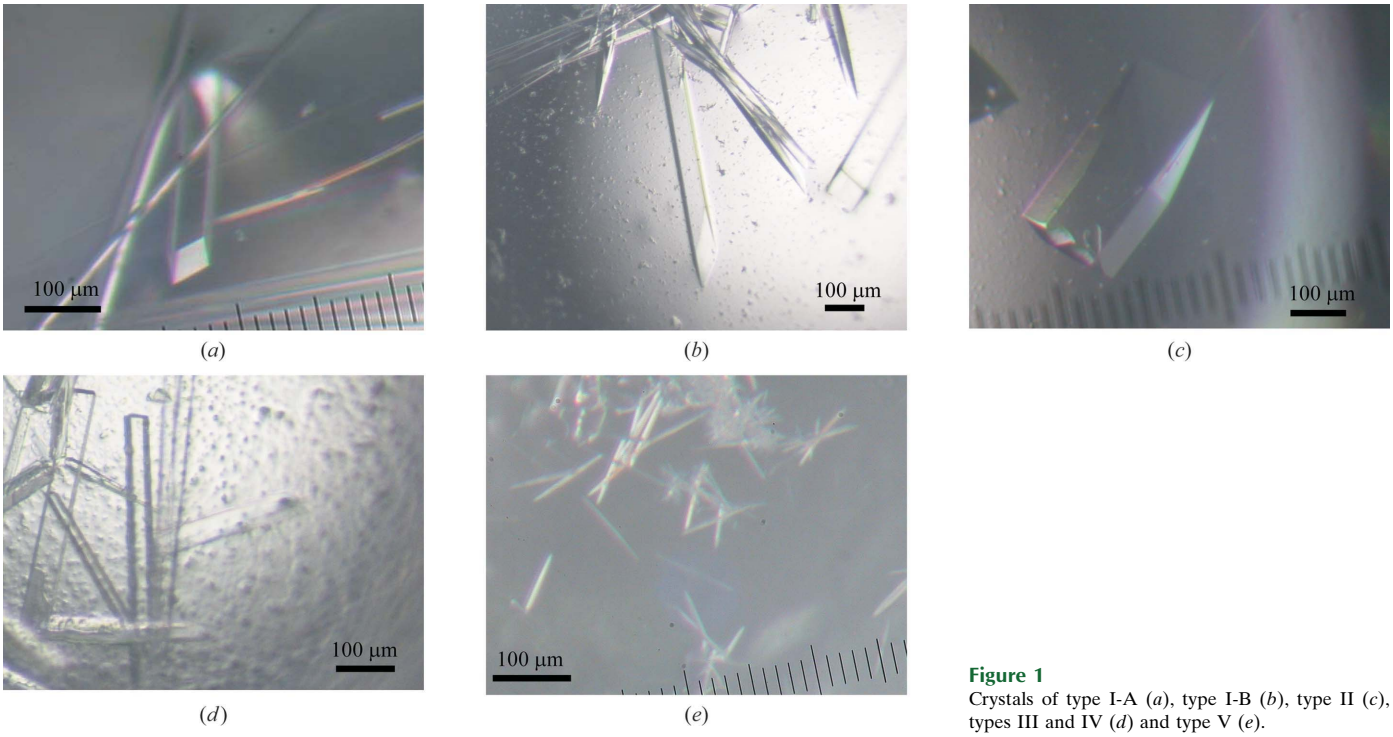

Figure 1
Crystals of type I-A (*a*), type I-B (*b*), type II (*c*), types III and IV (*d*) and type V (*e*).

Cambridge, Massachusetts, USA) pre-equilibrated with buffer *C*. The loaded column was washed with 25 ml buffer *C* and $CTD_{161–340}$ was eluted with 50 ml buffer *C* containing a linear NaCl gradient from 100 m*M* to 1 *M*. The protein was concentrated with an Amicon Ultra-10K concentrator (Millipore, Billerica, Massachusetts, USA) and applied onto a Superdex 75 10/30 gel-filtration column (GE Healthcare) pre-equilibrated with buffer *A*. The gel-filtration chromatogram indicated that the purified $CTD_{161–340}$ forms a dimer.

2.1.4. $CTD_{155–340}$. The cDNA for Pro155–Ile340 of Hdj1 with an initial methionine residue at the N-terminus ($CTD_{161–340}$) was amplified and subcloned as described for the preparation of the $CTD_{161–340}$ plasmid. The resultant plasmid was transformed into *E. coli* BL21 (DE3) pLysS cells. Expression and purification were performed as described for the purification of $CTD_{161–340}$.

2.2. Crystallization

All of the CTDs and the full-length Hdj1 were concentrated to the desired concentrations for crystallization experiments using Amicon Ultra-10K and Ultra-30K concentrators. Crystallization experiments were performed by the hanging-drop vapour-diffusion method.

2.2.1. $CTD_{161–340}$. Crystals of $CTD_{161–340}$ (type I-A crystals) were grown from an equivolume mixture of 10 mg ml^{-1} $CTD_{161–340}$ in buffer *A* and a reservoir solution consisting of 13%(*w*/*v*) PEG 3350 and 100 m*M* citrate buffer pH 6.0 at 293 K. Rod-shaped crystals appeared and grew to typical dimensions of 0.10 × 0.03 × 0.50 mm within 1 d (Fig. 1*a*). Crystals of $CTD_{161–340}$ in the presence of the C-terminal GPTIEEVD octapeptide of human Hsp70 (type I-B crystals) were grown from an equivolume mixture of 10 mg ml^{-1} $CTD_{161–340}$ solution containing 4 m*M* octapeptide at a molar ratio of 1:8.6 and a reservoir solution consisting of 18%(*w*/*v*) PEG 3350 and 100 m*M* citrate buffer pH 6.0 at 277 K. Rod-shaped type I-B crystals appeared and grew to typical dimensions of 0.07 × 0.03 × 0.80 mm within 1 d (Fig. 1*b*).

2.2.2. $CTD_{151–340}$. Crystals of $CTD_{151–340}$ (type II crystals) were grown from an equivolume mixture of 20 mg ml^{-1} $CTD_{151–340}$ in buffer *A* containing 4.5 m*M* octapeptide at a molar ratio of 1:4.8 and a reservoir solution consisting of 18%(*w*/*v*) PEG 3350 and 100 m*M* CHES pH 8.8 at 293 K. Rod-shaped type II crystals grew to typical dimensions of 0.05 × 0.15 × 0.60 mm within 1 d (Fig. 1*c*).

2.2.3. $CTD_{155–340}$. Type III and IV crystals of $CTD_{155–340}$ were grown under the same conditions as the type II crystals. Both crystal types were rod-shaped and grew to typical dimensions of 0.03 × 0.07 × 0.80 mm within 1 d (Fig. 1*d*).

2.2.4. Hdj1. Crystals of Hdj1 were grown from an equivolume mixture of 10 mg ml^{-1} Hdj1 in buffer *A* and a reservoir solution consisting of 1.3 *M* ammonium sulfate, 50 m*M* MES buffer pH 6.4 and 10 m*M* $MgCl_2$ at 293 K. Under these conditions, only clusters of needle-shaped crystals with a thickness of less than 0.005 mm could be obtained. A microseed stock solution was prepared from the clusters by crushing the crystals in 50 µl buffer *D* (1.1 *M* ammonium sulfate, 25 m*M* MES buffer pH 6.4, 5 m*M* $MgCl_2$, 10 m*M* sodium citrate and 50 m*M* NaCl) and this solution was diluted to 1 ml using buffer *D*. 3 µl of a 5 mg ml^{-1} Hdj1 solution that had been dialyzed against buffer *D* was mixed with 0.5 µl of the microseed stock solution. The mixtures were equilibrated against a reservoir solution consisting of 1.3 *M* ammonium sulfate, 25 m*M* MES buffer pH 6.4, 5 m*M* $MgCl_2$, 10 m*M* sodium citrate and 50 m*M* NaCl. Rod-shaped single crystals of Hdj1 (type V crystals) appeared and grew to typical dimensions of 0.01 × 0.01 × 0.15 mm within 2 d (Fig. 1*e*). The crystals were washed several times with the reservoir solution, dissolved in water and then analyzed by SDS–PAGE (Fig. 2). The PAGE results showed a single band with the same molecular weight as purified Hdj1.

2.3. Diffraction data collection and processing

All diffraction data were processed, integrated and scaled using the *HKL*-2000 package (Otwinowski & Minor, 1997). The self-rotation functions were computed using the program *MOLREP* implemented in the *CCP*4 package (Collaborative Computational Project, Number 4, 1994) based on the diffraction data to a maximum resolution of 4.0 Å. Diffraction data were also analyzed for pseudo-translational symmetry using *SFCHECK* (Vaguine *et al.*, 1999).

2.3.1. $CTD_{161–340}$. Type I-A and I-B crystals of $CTD_{161–340}$ soaked for a few seconds in reservoir solution containing 30% glycerol were flash-cooled to 95 K. Diffraction data were collected on BL-6A at the Photon Factory, Tsukuba, Japan. The type I-A and I-B crystals diffracted to 1.90 and 1.85 Å resolution, respectively.

2.3.2. $CTD_{151–340}$. Type II crystals were soaked for a few seconds in reservoir solution containing 15%(*w*/*v*) PEG 20 000 and 10%(*w*/*v*) PEG 400 and were flash-cooled to 120 K. The diffraction data were collected using a Cu rotating-anode X-ray generator and an R-AXIS IV detector (Rigaku, Tokyo, Japan). The type II crystal diffracted to 2.51 Å resolution.

2.3.3. $CTD_{155–340}$. Type III and IV crystals of $CTD_{155–340}$ were soaked for a few seconds in reservoir solution containing 15%(*w*/*v*) PEG 20 000 and 10%(*w*/*v*) PEG 400 and were flash-cooled to 100 K. The diffraction data were collected on BL38B1 at SPring-8, Harima, Japan. The type III and IV crystals diffracted to 1.90 and 2.80 Å resolution, respectively.

2.3.4. Hdj1. Type V crystals of Hdj1 were soaked for a few seconds in reservoir solution containing 30% glycerol and were flash-cooled to 95 K. Diffraction data were collected on BL-17A at the Photon Factory. The crystal diffracted to 3.8 Å resolution.

3. Results and discussion

The data-collection statistics of the diffraction data, together with the unit-cell parameters, are presented in Table 1. Complete diffraction data were collected for all of the CTD crystals, but not for Hdj1.

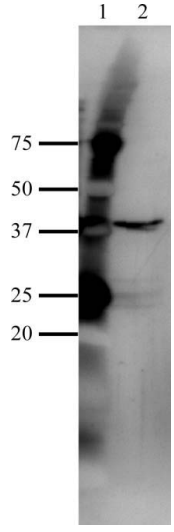

Figure 2
SDS–PAGE analysis of a full-length Hdj1 crystal. Lane 1, molecular-weight markers; molecular weights are labelled in kDa on the left. Lane 2, dissolved crystals of full-length Hdj1. Silver staining was used for protein detection.

Table 1
X-ray data-collection statistics.

Values in parentheses are for the highest resolution shell.

Crystal	Type I-A	Type I-B	Type II	Type III	Type IV	Type V
Construct	Asp161–Ile340	Asp161–Ile340	Ser151–Ile340	Pro155–Ile340	Pro155–Ile340	Met1–Ile340
Crystal data						
Space group	$P2_1$	$P2_1$	$C2$	$C2$	$C2$	$P2_1$
Unit-cell parameters						
a (Å)	103.3	104.7	111.1	111.1	193.1	106.3
b (Å)	40.9	41.1	50.9	51.3	40.6	41.0
c (Å)	62.7	62.9	90.2	90.2	128.6	95.3
β (°)	96.6	97.4	114.8	114.8	115.8	116.9
V_M (Å^3 Da^{-1})	3.21	3.28	2.70	2.76	2.68	2.40
Solvent content (%)	61.8	62.6	54.4	55.4	54.2	48.7
No. of protomers per ASU	2	2	2	2	4	2
Diffraction data statistics						
Wavelength (Å)	0.9780	0.9780	1.5418	0.9000	0.9000	0.9500
Resolution (Å)	102.6–2.05 (2.12–2.05)	103.7–1.85 (1.90–1.85)	81.9–2.51 (2.57–2.51)	81.9–2.10 (2.18–2.10)	115.5–2.80 (2.90–2.80)	50.0–3.90 (3.97–3.90)
No. of observed reflections	169938	389035	90145	230072	186082	22078
No. of unique reflections	33295	43147	14847	26399	22693	5038
Redundancy	5.1 (3.5)	9.0 (3.4)	6.1 (4.6)	8.7 (5.5)	8.2 (7.3)	4.4 (4.1)
Completeness (%)	99.1 (96.6)	99.1 (96.9)	98.2 (87.1)	99.7 (98.2)	99.9 (99.7)	72.2 (58.5)
$\langle I/\sigma(I)\rangle$	23.6 (3.3)	23.1 (1.5)	21.4 (3.3)	25.8 (3.0)	30.6 (4.1)	13.6 (6.3)
R_{merge}†	0.100 (0.420)	0.056 (0.482)	0.058 (0.386)	0.104 (0.408)	0.106 (0.391)	0.269 (0.499)

† $R_{merge} = \sum_{hkl}\sum_i |I_i(hkl) - \langle I(hkl)\rangle| / \sum_{hkl}\sum_i I_i(hkl)$.

The type I-A and type I-B crystals of $CTD_{161–340}$ both belonged to space group $P2_1$ and their unit-cell parameters are similar to each other, although the unit-cell volume of the type I-B crystal, which was grown in the presence of the octapeptide, is 2% larger than that of the type I-A crystal grown in the absence of the octapeptide. Type I-B crystals were obtained at a higher concentration of PEG 3350 than that used for type I-A crystals. This observation indicates that the octapeptide enhanced the solubility of $CTD_{161–340}$ and the type I-B crystals diffracted to a higher resolution than the type I-A crystals. These differences may have been caused by the formation of the $CTD_{161–340}$–octapeptide complex in the type I-B crystals; however, confirmation of the formation of a complex requires crystal structure determination. Assuming the presence of one dimer of $CTD_{161–340}$ per asymmetric unit, the V_M values are 3.21 and 3.28 Å^3 Da^{-1} and the calculated solvent contents are 61.8 and 62.6%, respectively (Matthews, 1968). This is consistent with the presence of a noncrystallographic twofold axis, as indicated by the self-rotation functions, in which clear peaks 13σ and 17σ above the average were observed at (θ = 18°, φ = 0°) in the κ = 180° section for the type I-A and I-B crystals, respectively.

The type II crystals of $CTD_{151–340}$ and the type III crystals of $CTD_{155–340}$ belonged to space group $C2$ and their unit-cell parameters are nearly identical. Assuming the presence of one dimeric CTD per asymmetric unit, their V_M values are 2.70 and 2.76 Å^3 Da^{-1} and their calculated solvent contents are 54.4 and 55.4%, respectively. Nevertheless, no clear peak could be observed in the κ = 180° section of the self-rotation function for either type of crystal. The CTD of Hsp40 consists of three subdomains (Sha *et al.*, 2000; Hu *et al.*, 2008). The absence of noncrystallographic twofold symmetry may be a consequence of the subdomain arrangements of the two protomers of $CTD_{151–340}$ differing from each other in these types of crystals. Alternatively, the noncrystallographic twofold axis may be parallel to the crystallographic twofold or 2_1 screw axes.

The type IV crystal belonged to space group $C2$ and the volume of the asymmetric unit was the largest of the CTD crystals examined. Assuming the presence of two dimers of $CTD_{155–340}$ per asymmetric unit, the V_M value is 2.68 Å^3 Da^{-1} and the calculated solvent content is 54.2%. No clear peak could be observed in the κ = 180° section of the self-rotation function. In a native Patterson map, a non-origin peak was observed at (0.500, 0.410, 0.500), indicating the presence of pseudo-translational symmetry. The two dimers of $CTD_{155–340}$ in the asymmetric unit, as suggested by the V_M value, may be related by this pseudo-translational symmetry.

Of the three kinds of CTDs, those with the longer N-termini, $CTD_{151–340}$ and $CTD_{155–340}$, only crystallized in the presence of the octapeptide and under alkaline conditions around pH 9. In contrast, the CTD with the shortest N-terminus, $CTD_{161–340}$, crystallized under slightly acidic conditions at pH 6 and crystallized in both the presence and the absence of the octapeptide. The length of the N-terminus also affected the reproducibility of the crystals: type I-A and I-B crystals of $CTD_{161–340}$ diffracted to the maximum resolution shown in Table 1 with nearly 100% reproducibility, whereas the reproducibilities of the type II crystal of $CTD_{151–340}$ and the type III and IV crystals of $CTD_{155–340}$ that diffracted to maximum resolution were less than 5%.

Determination of the structure of the type I-A crystal by the single isomorphous replacement method with anomalous scattering and its crystallographic refinement are in progress. Determination of the structures of the type I-B, II, III and IV crystals were performed by the molecular-replacement method using the type I-A crystal structure as a search model. Inspection of the preliminary electron-density maps revealed that the octapeptides were bound to two discrete sites, 1 and 2, as shown in Supplementary Fig. S1[1]. Crystallographic refinements of these structures are under way.

Despite the weak diffraction of the type V crystals, the diffraction data revealed that the crystals belonged to space group $P2_1$; assuming the presence of one dimer of Hdj1 per asymmetric unit, the V_M value is 2.40 Å^3 Da^{-1} and the calculated solvent content is 48.7%. This is the only reported case in which full-length Hsp40 has been crystallized. Although the resolution and completeness of the diffraction data of the type V crystal are low, structure determination of the type V crystal may be possible using the molecular-replacement method. The crystal structure should provide insight into the domain arrangement of full-length Hsp40.

[1] Supplementary material has been deposited in the IUCr electronic archive (Reference: UO5011).

The cDNA of the human Hsp40 Hdj1 was kindly provided by Professor K. Ohtsuka of Chubu University. This work was supported by Grants-in-Aid from the Japanese Ministry of Education, Culture, Sports, Science and Technology (MEXT) as well as a Protein 3000 grant (YS) and in part by the Global COE Program 'Medical System Innovation on Multidisciplinary Integration' from MEXT, Japan (HS). The synchrotron-radiation experiments were performed under the approval of the Photon Factory Program Advisory Committee (Proposal No. 2008G141) and of the Japan Synchrotron Radiation Research Institute (JASRI; Proposal No. 2008B1179).

References

Bukau, B. & Horwich, A. L. (1998). *Cell*, **92**, 351–366.
Cheetham, M. E. & Caplan, A. J. (1998). *Cell Stress Chaperone*, **3**, 28–36.
Collaborative Computational Project, Number 4 (1994). *Acta Cryst.* D**50**, 760–763.
Freeman, B. C., Myers, M. P., Schumacher, R. & Morimoto, R. I. (1995). *EMBO J.* **14**, 2281–2292.
Frydman, J., Nimmesgern, E., Ohtsuka, K. & Hartl, F. U. (1994). *Nature (London)*, **370**, 111–117.
Han, W. & Christen, P. (2003). *J. Biol. Chem.* **278**, 19038–19043.
Hartl, F. U. & Hayar-Hartl, M. (2002). *Science*, **295**, 1852–1858.
Holstein, S. E., Ungewickell, H. & Ungewickell, E. (1996). *J. Cell Biol.* **135**, 925–937.
Hu, J., Wu, Y., Li, J., Qian, X., Fu, Z. & Sha, B. (2008). *BMC Struct. Biol.* **8**, 3.
Matthews, B. W. (1968). *J. Mol. Biol.* **33**, 491–497.
Otwinowski, Z. & Minor, W. (1997). *Methods Enzymol.* **276**, 344–358.
Sha, B., Lee, S. & Cyr, D. M. (2000). *Structure*, **8**, 799–807.
Vaguine, A. A., Richelle, J. & Wodak, S. J. (1999). *Acta Cryst.* D**55**, 191–205.

Supplementary Figure S1

F_o - F_c difference Fourier maps of the octapeptides. The maps are calculated at maximum resolution shown in Table 1 using the model obtained from the molecular-replacement method by MOLREP. The maps at sites 1 and 2 are coloured in blue and green, respectively. Preliminary CTD and octapeptide models are shown as C^{α} traces in orange and magenta, respectively. (*a*) Site 1 of type I-B crystal, contoured at 1.5σ. (*b*) Site 2 of type I-B crystal, contoured at 1.5σ. (*c*) Site 1 of type II crystal, contoured at 1.6σ. (*d*) Site 2 of type I-B crystal, contoured at 1.6σ. (*e*) Site 1 of type III crystal, contoured at 1.5σ. (*f*) Site 2 of type III crystal, contoured at 1.3σ. (*g*) Site 1 of type IV crystal, contoured at 1.5σ. (*h*) Site 2 of type IV crystal, contoured at 1.5σ.

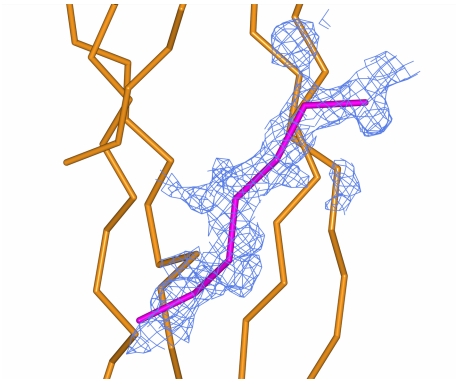

(*a*)

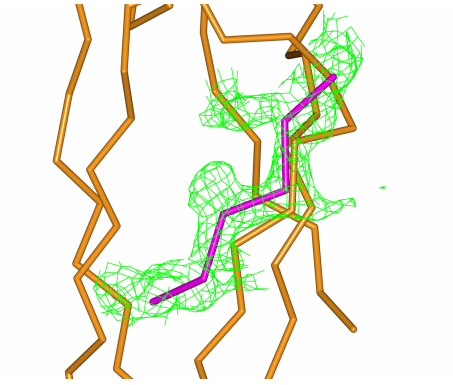

(*b*)

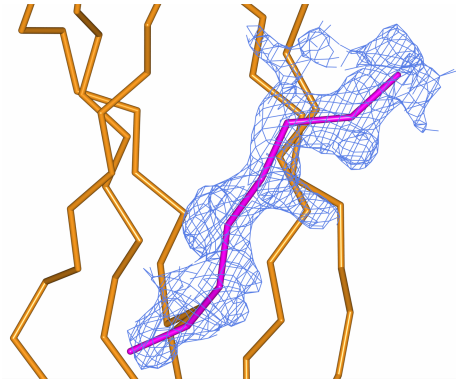

(*c*)

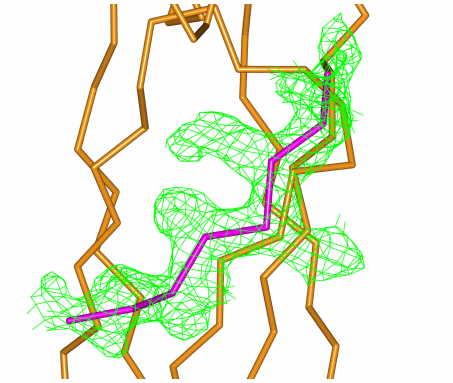

(*d*)

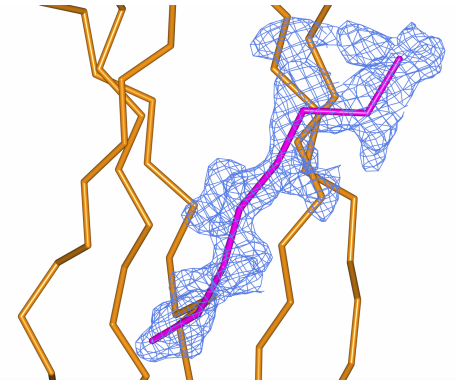

(*e*)

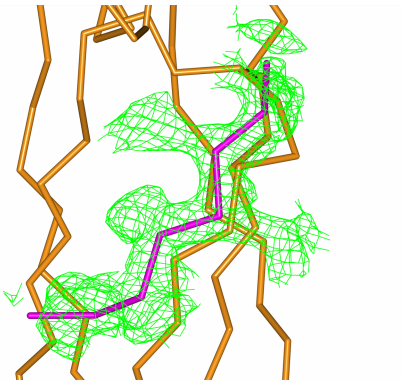

(*f*)

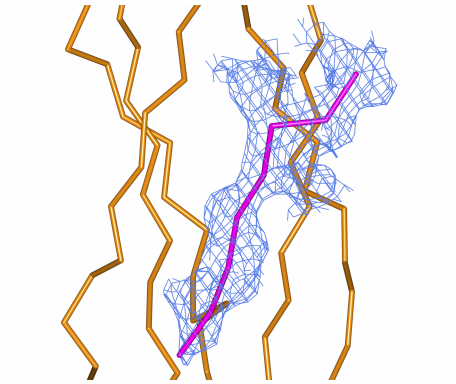

(*g*)

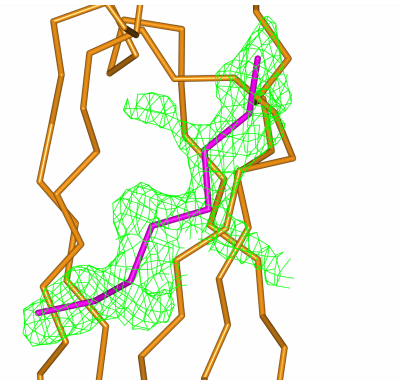

(*h*)